Generation of 88 as Isolated Attosecond Pulses with Double Optical Gating *

Xiaowei Wang(王小伟)[1], Li Wang(王力)[1], Fan Xiao(肖凡)[1], Dongwen Zhang(张栋文)[1], Zhihui Lü(吕治辉)[1], Jianmin Yuan(袁建民)[1,2,3], Zengxiu Zhao(赵增秀)[1]**

[1]*Department of Physics, National University of Defense Technology, Changsha 410073*
[2]*Department of Physics, Graduate School of China Academy of Engineering Physics, Beijing 100193*
[3]*IFSA Collaborative Innovation Center, Shanghai Jiao Tong University, Shanghai 200240*

(Received 6 December 2019)

Isolated attosecond pulses with a duration of 88 as are generated in the spectral range of 29–72 eV using double optical gating technique. The gate width is set to be shorter than half the optical cycle to avoid carrier envelop phase stabilization of the 4.2 fs driving laser pulses centered at 800 nm. The attosecond pulse duration is measured with the technique of frequency resolved optical gating for complete reconstruction of attosecond bursts.

PACS: 32.30.Rj, 42.65.Re, 32.80.Fb DOI: 10.1088/0256-307X/37/2/023201

With ultra-broadband spectrums and ultrashort time scales, isolated attosecond pulses (IAP) have been proven to be a powerful tool to probe the ultrafast electron dynamics in atoms,[1,2] molecules,[3–5] and condensed matter.[6,7] The development of ultrashort IAP sources is the key to attosecond physics and has cost a lot of effort. Great progress has been made in the last decade and IAPs as short as 2 units of atomic time (1 a.u.=24.2 as) have been demonstrated.[8,9]

Attosecond pulse trains (APT) can be directly generated via high-order harmonic generation (HHG), in which the three step dynamics (ionization, acceleration and recombination) of electrons give birth to an attosecond pulse in every half cycle of the driving laser.[10] However, extracting an IAP out of the APT needs various gating methods,[11] such as ionization gating (IG),[12,13] amplitude gating (AG),[14] polarization gating (PG),[15,16] double optical gating (DOG),[17,18] and attosecond lighthouse (ALH).[19,20] The gating methods manage to shutdown most of the electron recombination process by finely controlling the electric field of the driving laser, including the electric field strength (IG, AG), pulse duration (AG), polarization (PG, DOG) and even the wavefront (ALH). The carrier envelop phase (CEP), which determines the shape of the electric field, is usually required to be stable. However, this will be unnecessary if the gate width is kept narrow enough.[21]

To reach 10^{14}–10^{15} W/cm^2 intensity for HHG, amplified mini-Joule level femtosecond pulses are usually desired. Few-cycle 800 nm near infrared (NIR) pulses are popular driving pulses for IAP generation. However, with the advance of few-cycle middle infrared laser (Mid-IR) pulse generation,[22–24] longer wavelength driver has become favorable recently because a higher photon energy and wider IAP bandwidth can be achieved due to the quadratic scaling of the ponderomotive energy with wavelength. This was termed the second generation of attosecond light sources,[8] while the NIR produced IAPs are the first generation. Although much shorter IAPs have been demonstrated with Mid-IR femtosecond pulses, the first generation IAPs have their own advantages: (1) The few-cycle NIR pulses as well as the corresponding gating techniques are well-developed. (2) The intrinsic chirp is easier to compensate due to narrower bandwidth and lower photon energy. (3) The low-lying photon energy is very suitable for valence electron dynamics measurement. (4) The conversion efficiency is higher for driving laser pulses with shorter wavelength. Therefore, generating relatively short IAPs in low energy range is still valuable. In this Letter, we report the generation of 88 attosecond extreme ultraviolet (XUV) IAPs in the energy range of 29–72 eV with CEP unstabilized few-cycle NIR laser pulses.

The laser source of our experiments was a Ti:sapphire based chirped pulse amplification (CPA) system (Femtopower Pro HE) which outputs 4.2 mJ, 25 fs pulses centered at 800 nm with 1 kHz repetition rate. The pulses were then fed into a 1-m-long 2-bar-helium filled hollow-core fiber for spectral broadening. The gas pressure at the entrance of the fiber was kept at 2–3 mbar by differential pumping to avoid ionization induced energy drop and spectra blueshift. Therefore, throughput as high as 50% was achieved. The broadened spectra covered a very wide wavelength range from below 600 nm to above 900 nm, as shown in Fig. 1(a). The dispersion was then compensated for with chirped mirrors. The pulse duration

*Supported by the National Key Research and Development Program of China under Grant No. 2019YFA0307703, the Major Research Plan of the National Natural Science Foundation of China under Grant No. 91850201, and the National Natural Science Foundation of China under Grant No. 11974426.

**Corresponding author. Email: zhaozengxiu@nudt.edu.cn

© 2020 Chinese Physical Society and IOP Publishing Ltd

was measured with a fringe resolved autocorrelator (FRAC). The full width of half maximum (FWHM) of the autocorrelation signal is 8 fs as shown in Fig. 1(b), the pulse duration was then deduced as 8/1.9=4.2 fs if sech^2 temporal shape is assumed.

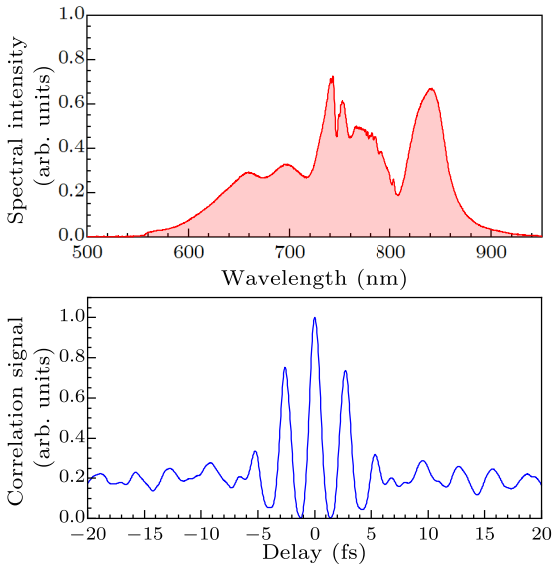

Fig. 1. The spectrum (a) and FRAC measurement (b) of few-cycle NIR pulses. The FWHM of the autocorrelation signal is 8 fs, so the duration of NIR pulses is estimated to be 4.2 fs.

Sub-5 fs pulses are qualified for almost all the gating methods. DOG was used in this work to produce broadband IAPs since it can cover both the plateau and cutoff photons. Another important reason is that DOG can waive the requirement of CEP stabilization, which could be troublesome for time-consuming attosecond streak camera measurements. In DOG scheme, two quartz plates and one BBO crystal are used to form the proper gating. The first quartz plate introduces a certain delay T_d between the two counter-rotating pulses, thereby determines the gate width t_G for a given input pulse with a duration of τ_p:[18]

$$t_\mathrm{G} \approx \varepsilon \frac{\xi_\mathrm{th}}{\ln 2} \frac{\tau_\mathrm{p}^2}{T_\mathrm{d}}, \tag{1}$$

where $\xi_\mathrm{th} = 0.2$ is the threshold ellipticity, ε is the ellipticity of the counter-rotating pulses. For DOG, ε is 1. Thus we can change the thickness of the first quartz plate to make sure that the gate width is much shorter than the temporal interval of the adjacent attosecond pulses, so that only one IAP can be generated no matter what the CEP is. A safe gate width is $t_\mathrm{G} = 1$ fs, which is short enough for gating and long enough for the excursion of short trajectory electrons. Note that not every value of T_d calculated from Eq. (1) is acceptable, since T_d has to be integer multiples of the driving laser period T_0 so that the linear electric field in the gate has the same polarization as the input pulse. If we set $T_\mathrm{d} = 2T_0 = 5.4$ fs, the resulted $t_\mathrm{G} = 0.98$ fs is viable.

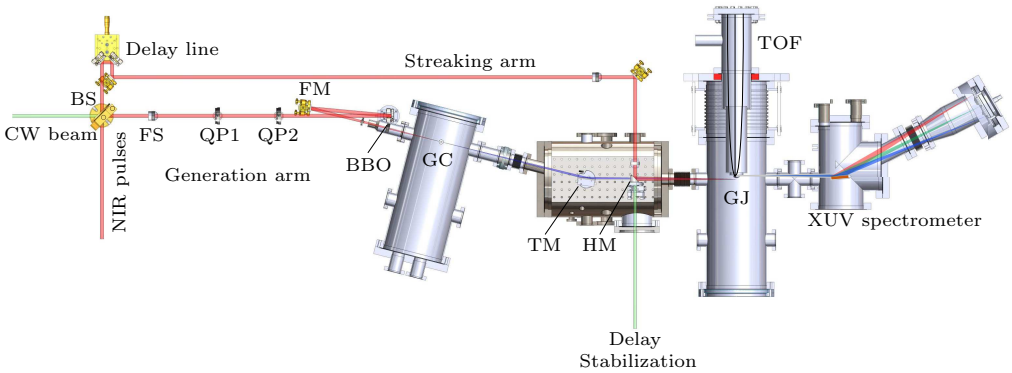

Fig. 2. Experimental setup. The 1.8 mJ, 4.2 fs NIR pulses were split by a 50 : 50 beam splitter (BS). The DOG optics (QP1, QP2 and BBO) formed a 0.98 fs gate for isolated attosecond pulse generation in neon filled gas cell (GC). The streaking pulses and the isolated attosecond pulses were recombined on a hole mirror (HM) and focused on a gas jet (GJ) to perform FROG-CRAB measurements. The IAP spectra can also be measured by the XUV spectrometer attached after the detection chamber.

The IAP generation and characterization experiments were carried out with a Mach–Zehnder interferometer based pump-probe layout as shown in Fig. 2. The 1.8 mJ, 4.2 fs few-cycle NIR pulses were split by a 50 : 50 beamsplitter into the generation and streaking pulses. The generation pulses were orthogonally split and delayed by the first 180-μm-thick quartz plate, which generated 0.98 fs gate width (as discussed earlier). The second 440-μm quartz plate together with the 141 μm β-beta-barium borate (BBO) crystal acted as a zero-order quarter wave plate to form two counter-rotating electric field. The weak second harmonic generated by BBO broke the symmetry of the fundamental electric field, thus increased the time interval of adjacent attosecond pulses from half cycle to full cycle. Then the pulses were focused by an $f = 500$ mm spherical silver mirror onto a neon gas cell with pressure-length product of 80 mbar·mm for IAP generation. The peak intensity of the driving field is tuned to be 6×10^{14} W/cm^2 with an iris. A 200-nm-thick alu-

minum foil was put afterwards to block the residual NIR pulses and to compensate the intrinsic chirp of attosecond pulses. The IAPs and streaking laser pulses were focused by a toroidal mirror ($f = 250$ mm) and a plano-convex lens ($f = 400$ mm), respectively and recombined by a hole-drilled mirror. The grazing incident toroidal reflector is capable of handling much broader IAPs than the two-segment Mo/Si multilayer mirrors used in previous research.[25]

A neon gas jet with backing pressure of 0.9 bar was placed right on the focus of the recombined XUV-NIR pulses to perform temporal characterization with frequency resolved optical gating for complete characterization of attosecond bursts (FROG-CRAB) technique.[26] The energy distribution of photoelectrons were measured with a 350-mm-long time-of-flight (TOF) electron spectrometer (ETF11, STEFAN KAESDORF). The signal from the TOF detector was digitized with 50 ps time resolution by a fast oscilloscope (Tektronix 7354 C). A home-made XUV spectrometer[27] is placed after the detection chamber to measure the IAP spectra. The delay between the XUV and NIR pulses was actively stabilized and precisely scanned by monitoring the interference fringes of a 532 nm continuous wave (CW) which co-propagated through both arms of the Mach–Zehnder interferometer.[28]

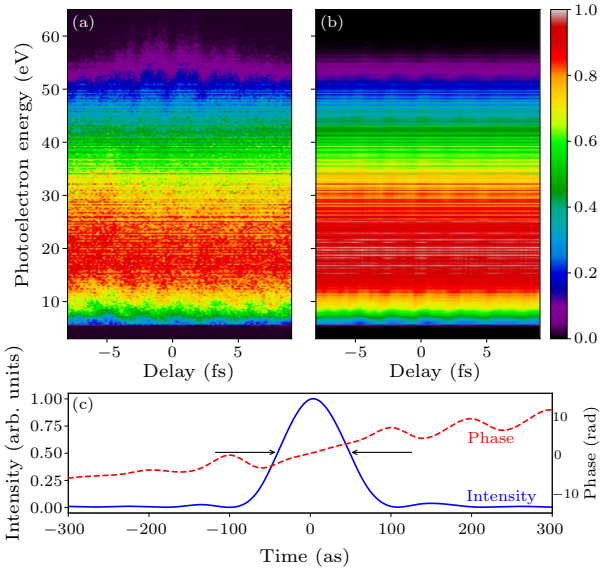

Fig. 3. The measured FROG-CRAB trace (a), reconstructed FROG-CRAB trace (b) and the retrieved IAP pulse temporal profile (solid line) and phase (dashed line) (c). The reconstructed trace did not reproduce the asymmetric energy streaking shift due to CMA.

During the IAP characterization, electron spectra were integrated for 80000 shots at each delay between the NIR pulses and XUV pulses. The electrons count rate was 1.4 electrons per pulse, so no space charge effect was expected in the electron energy spectra measurement. The delay was scanned through a time window of 17 fs with step size of 141 as. The measured FROG-CRAB trace is shown in Fig. 3(a). The photoelectron was centered at 20 eV and covered a wide spectra range from 8 eV to 52 eV. The photon electrons with kinetic energy W experienced an energy streaking shift by the NIR laser field $E_{\rm L}(t)$ with central frequency of $\omega_{\rm L}$ through the gate phase $e^{i(\phi_1+\phi_2+\phi_3)}$, where $\phi_2 = \sqrt{2W}E_{\rm L}(t)/\omega_{\rm L}^2$ is the dominate term,[26] the energy streaking shift δE can be estimated by

$$\delta E = \left|\frac{\partial\phi}{\partial d}\right|_{\max} \propto \sqrt{W}, \tag{2}$$

so the streaking shift of the upper edge electrons should be 2.5 times larger than that of the lower edge electrons, as the case shown in Fig. 3(a).

The retrieval was carried out with principal components generalized projections algorithm (PCGPA),[26,29] in which central momentum approximation (CMA) has to be made to separate time and energy variables so that fast Fourier transform (FFT) algorithm can apply. The reconstructed trace is shown in Fig. 3(b). Compared to the experimental trace, a significant discrepancy in the reconstructed trace is that the energy shift for high energy and low energy electrons is symmetric, which resulted from the CMA. However, the retrieved result is still trustworthy because CMA has proven to be capable of working with even large bandwidth IAPs.[30] The retrieved IAP temporal profile is shown in Fig. 3(c), which suggests 88.5 as IAP pulses were generated.

In conclusion, by setting the gate width to be 0.98 fs, we generate 88.5 as IAPs in the energy range of 29–72 eV using CEP unstabilized 4.2 fs NIR laser pulses with the help of DOG gating technique. With low photon energy and relatively short time scale, the IAPs are suitable to perform time resolved measurements for valence shell/outer shell electrons in atoms, molecules and solids.

References

[1] Chini M, Wang X W, Cheng Y, Wu Y, Zhao D, Telnov D A, Chu S I and Chang Z 2013 *Sci. Rep.* **3** 1105
[2] Ossiander M, Siegrist F, Shirvanyan V, Pazourek R, Sommer A, Latka T, Guggenmos A, Nagele S, Feist J, Burgdörfer J, Kienberger R and Schultze M 2017 *Nat. Phys.* **13** 280
[3] Lépine F, Ivanov M Y and Vrakking M J J 2014 *Nat. Photon.* **8** 195
[4] Nisoli M, Decleva P, Calegari F, Palacios A and Martín F 2017 *Chem. Rev.* **117** 10760
[5] Zhang B, Zhao J and Zhao Z X 2018 *Chin. Phys. Lett.* **35** 043201
[6] Ossiander M, Riemensberger J, Neppl S, Mittermair M, Schäffer M, Duensing A, Wagner M S, Heider R, Wurzer M, Gerl M, Schnitzenbaumer M, Barth J V, Libisch F, Lemell C, Burgdörfer J, Feulner P and Kienberger R 2018 *Nature* **561** 374
[7] Mashiko H, Chisuga Y, Katayama I, Oguri K, Masuda H, Takeda J and Gotoh H 2018 *Nat. Commun.* **9** 1468

[8] Li J, Ren X, Yin Y, Zhao K, Chew A, Cheng Y, Cunningham E, Wang Y, Hu S, Wu Y, Chini M and Chang Z 2017 *Nat. Commun.* **8** 1
[9] Gaumnitz T, Jain A, Pertot Y, Huppert M, Jordan I, Ardana-Lamas F and Wörner H J 2017 *Opt. Express* **25** 27506
[10] Corkum P B 1993 *Phys. Rev. Lett.* **71** 1994
[11] Chini M, Zhao K and Chang Z 2014 *Nat. Photon.* **8** 178
[12] Jullien A, Pfeifer T, Abel M J, Nagel P M, Bell M J, Neumark D M and Leone S R 2008 *Appl. Phys. B* **93** 433
[13] Abel M J, Pfeifer T, Nagel P M, Boutu W, Bell M J, Steiner C P, Neumark D M and Leone S R 2009 *Chem. Phys.* **366** 9
[14] Goulielmakis E, Schultze M, Hofstetter M, Yakovlev V S, Gagnon J, Uiberacker M, Aquila A L, Gullikson E M, Attwood D T, Kienberger R, Krausz F and Kleineberg U 2008 *Science* **320** 1614
[15] Corkum P B, Burnett N H and Ivanov M Y 1994 *Opt. Lett.* **19** 1870
[16] 2006 *Nat. Phys.* **2** 319
[17] Mashiko H, Gilbertson S, Li C, Khan S D, Shakya M M, Moon E and Chang Z 2008 *Phys. Rev. Lett.* **100** 103906
[18] Feng X M, Gilbertson S, Mashiko H, Wang H, Khan S D, Chini M, Wu Y, Zhao K and Chang Z 2009 *Phys. Rev. Lett.* **103** 183901
[19] Vincenti H and Quéré F 2012 *Phys. Rev. Lett.* **108** 113904
[20] Kim K T, Zhang C, Ruchon T, Hergott J F, Auguste T, Villeneuve D M, Corkum P B and Quéré F 2013 *Nat. Photon.* **7** 651
[21] Gilbertson S, Khan S D, Wu Y, Chini M and Chang Z 2010 *Phys. Rev. Lett.* **105** 093902
[22] Shumakova V, Malevich P, Ališauskas S, Voronin A, Zheltikov A M, Faccio D, Kartashov D, Baltuška A and Pugžlys A 2016 *Nat. Commun.* **7** 12877
[23] Liang H, Krogen P, Wang Z, Park H, Kroh T, Zawilski K, Schunemann P, Moses J, DiMauro L F, Kärtner F X and Hong K H 2017 *Nat. Commun.* **8** 141
[24] Yin Y, Ren X, Chew A, Li J, Wang Y, Zhuang F, Wu Y and Chang Z 2017 *Sci. Rep.* **7** 11097
[25] Zhan M J, Ye P, Teng H, He X K, Zhang W, Zhong S Y, Wang L F, Yun C X and Wei Z Y 2013 *Chin. Phys. Lett.* **30** 093201
[26] Mairesse Y and Quéré F 2005 *Phys. Rev. A* **71** 011401
[27] Wang X, Chini M, Cheng Y, Wu Y and Chang Z 2013 *Appl. Opt.* **52** 323
[28] Chini M, Mashiko H, Wang H, Chen S, Yun C, Scott S, Gilbertson S and Chang Z 2009 *Opt. Express* **17** 21459
[29] Kane D J, Rodriguez G, Taylor A J and Clement T S 1997 *J. Opt. Soc. Am. B* **14** 935
[30] Zhao K, Zhang Q, Chini M, Wu Y, Wang X and Chang Z 2012 *Opt. Lett.* **37** 3891